DOI: 10.1021/jm901727j

Journal of Medicinal Chemistry Article

Photooxidation and Phototoxicity of π-Extended Squaraines

Valentina Rapozzi,[†] Luca Beverina,[‡] Patrizio Salice,[‡] Giorgio A. Pagani,[‡] Monica Camerin,[§] and Luigi E. Xodo*[,†]

[†]*Department of Biomedical Science and Technology, University of Udine, P.le Kolbe 4, I-33100 Udine, Italy,* [‡]*Department of Materials Science and INSTM, University of Milano-Bicocca, via Cozzi 53 I-20125 Milano, Italy, and* [§]*Department of Biology, Via U. Bassi 58/B, University of Padova, 35131 Padova, Italy*

Received November 23, 2009

This paper describes the synthesis of π-extended squaraines and their photooxidation properties and gives an in-depth characterization of these molecules as photosensitizing agents. Squaraines show a strong absorption in the tissue transparency window (600−800 nm), and upon irradiation, they undergo a photooxidation process, leading to the formation of peroxide and hydroperoxide radicals according to a type I radical chain process. Confocal laser microscopy demonstrates that the designed squaraines efficiently internalize in the cytoplasm and not in the nucleus of the cell. In the dark, they are scarcely cytotoxic, but after irradition, they promote a strong dose-dependent phototoxic effect in four different cancer cells. In HeLa and MCF-7 cells, squaraines **4** and **5**, thanks to their hydrocarbon tails, associate to the membranes and induce lipid peroxidation, as indicated by a marked increase of malonyldialdehyde after photodynamic treatment, in agreement with in vitro photooxidation studies. FACS, caspase-3/7 assays and time-lapse microscopy demonstrate that the designed squaraines cause cell death primarily by necrosis.

Introduction

The condensation of electron-rich compounds with squaric acid gives rise to a variety of molecules known as squaraines.[1−4] As these molecules are characterized by an intense absorption between 600 and 800 nm—where tissues are fairly transparent to light—they have a potential as photosensitizers in photodynamic therapy (PDT).[5−8] In addition, squaraines have been proposed as near-infrared dyes for the determination of low molecular mass aminothiols in human plasma.[9] PDT is a therapeutic modality used in a number of diseases including psoriasis, age-related macular degeneration, and cancer.[10−13] It involves the systemic or topic administration of a photosensitizer that, after excitation, produces singlet oxygen and/or reactive oxygen species (ROS), which cause photodamage to cancer cells.[14,15] One of the main goals in PDT research is the discovery of new photosensitizers possessing minimal dark cytotoxycity, high photodynamic properties, preferential retention in diseased rather than in healthy tissues, chemical stability, and a good cellular uptake.[13,16,17] Although a number of new phosensitizers have been proposed,[18−25] the most widely used in the clinic is a mixture of hematoporphyrines.[12] It is used for different cancers, but its absorption above 600 nm is weak.[10] Thus, there is great interest to search for new and more efficient PDT molecules. In this paper, we report the synthesis and photodynamic properties of two symmetric squaraines, namely, **4** and **5** (Scheme 1), both of which have *N*-alkylbenzothiazole residues as end-capping groups. The two squaraines each contain two C-6 hydrocarbon chains that might favor their association to the cell membranes. Little is known about the photosensitizing properties of squaraines in cell cultures. Ramaiah et al.[7] have reported that halogenated monosquaraines significantly reduce the clonogenicity of AS52 Chinese hamster ovary cells after photoactivation. Gayathri Devi et al.[26] have shown that a tetraiodo-squaraine caused a reduction of tumor volume and a reversal of biochemical markers to near-normal levels in mice bearing a skin tumor, treated with tetraiodo squaraine and exposed to a 1000 W halogen lamp. In this study, we report on the photobleaching and photooxidation of mono- and bis-squaraines as well as their photosensitizing properties in four different cancer cells. We provide strong evidence that the mechanism of cell death promoted by this new class of photosensitizers is mediated by lipid peroxidation.

Results and Discussion

Synthesis Squaraines 4 and 5. The bis-squaraine **4** was prepared according to Scheme 1a. In brief, commercially available 2,2′:5′,2″-terthiophene (**1**) was treated with 2 equiv of BuLi at 0 °C in tetrahydrofuran (THF). The lithiated terthiophene was subsequently treated with 2 equiv of commercially available butylsquarate to give, after acidic workup, bis-semisquarate (**2**). Acidic hydrolysis in refluxing AcOH and in the presence of aqueous HCl gave the bis-semisquaraine (**3**), which was finally converted in the bis-squaraine (**4**) as recently reported.[27] The analytically pure compound was obtained as a golden brown precipitate. Squaraine **5** was, instead, prepared following the method described by Santos and co-workers by refluxing a BuOH/pyridine suspension of the benzothiazolium salt and squaric acid under azeotropic distillation of the water formed (Scheme 1b).[5]Squaraines **4** and **5** are characterized by an intense absorption band between 550 and 750 nm, and because of this property, they have the potential in PDT as a photosensitizer (Figure 1). Their absorption and emission properties in different organic solvents are reported in Table 1.

Photobleaching and Photooxidation of Squaraines. When **5** is dissolved in air-equilibrated acetonitrile and irradiated

*To whom correspondence should be addressed. Tel: +39.0432.494395. Fax: +39.0432.494301. E-mail: luigi.xodo@uniud.it.

 Published on Web 02/04/2010

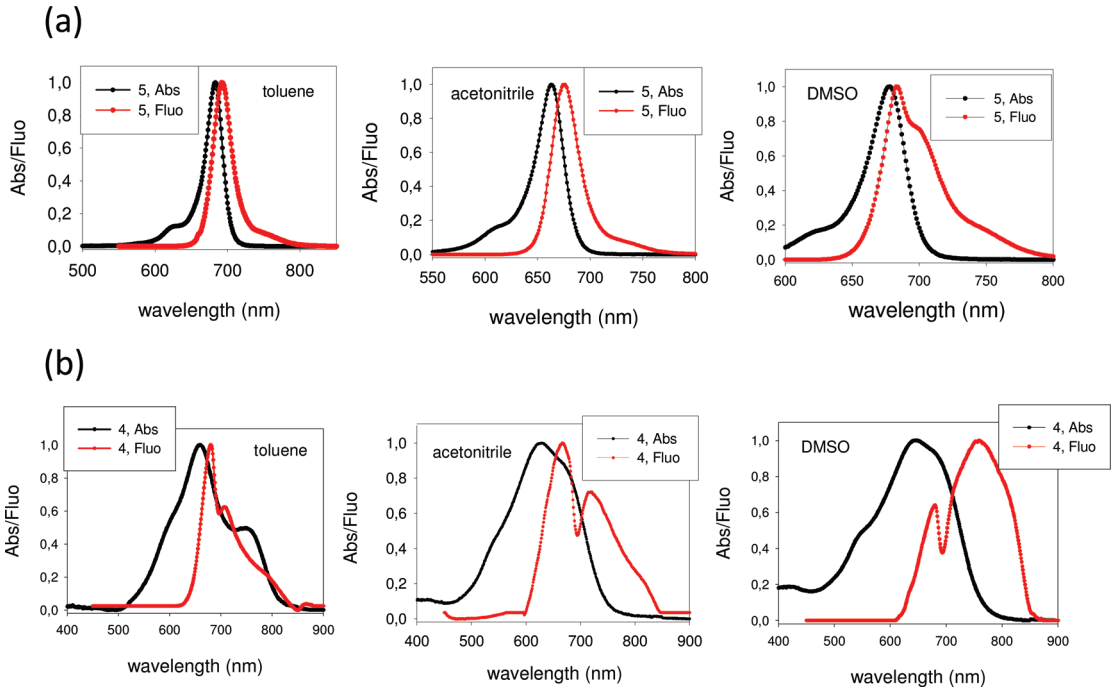

Figure 1. Absorption (black line) and fluorescence (red line) spectra for squaraines **4** and **5** in different organic solvents.

Scheme 1. (a) Synthetic Route to Bis-squarine **4** and (b) Synthetic Route to Squaraine **5**

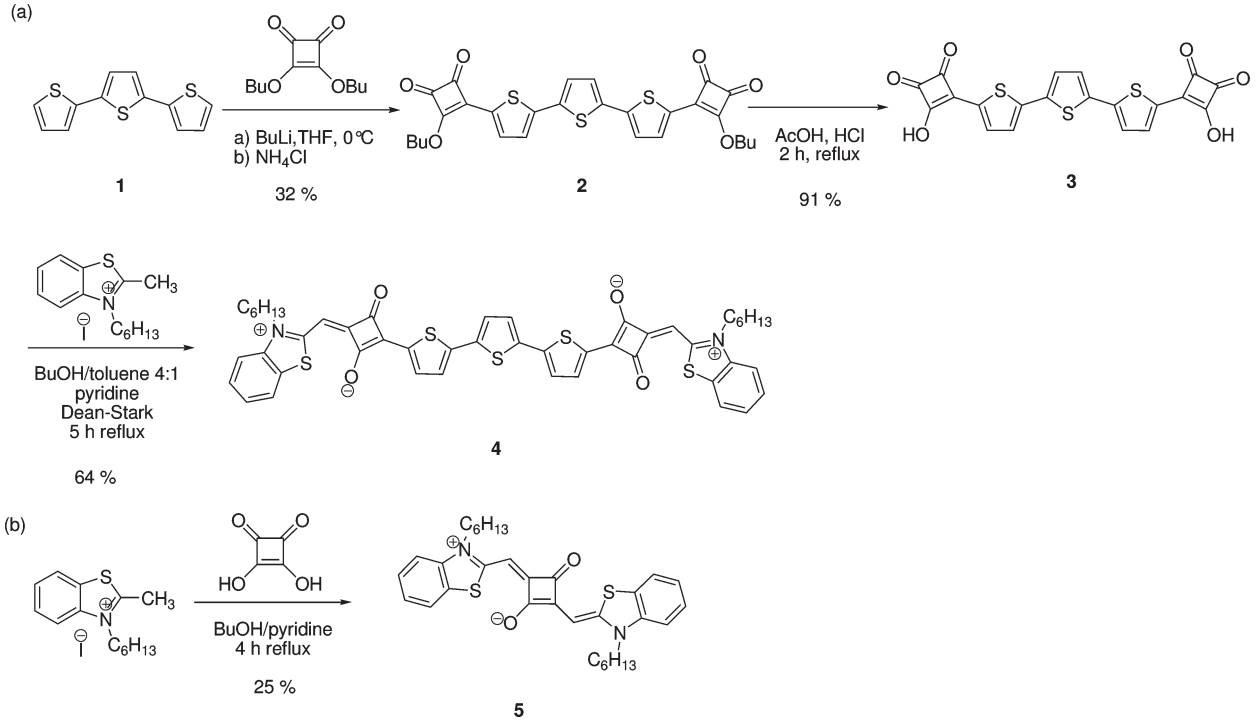

with a laser or halogen lamp, it undergoes extensive degradation (Figure 2). This behavior does not occur when acetonitrile is saturated with nitrogen, and it slowly occurs when air-equilibrated low polar solvents such as toluene are used. We rationalized this behavior in terms of the formation of a charge-transfer encounter complex between the squaraine and the molecular oxygen, eventually evolving in the formation of different chemical species. To unveil the photochemical mechanism involved, we analyzed a completely sun-bleached solution of **5** in air-equilibrated acetonitrile by GC-MS. We observed, among other species, the formation of 3-hexylbenzo[*d*]thiazol-2(3*H*)-one (3-HBT).[a] We speculate that the formation of 3-HBT is in agreement with the chemistry of photooxygenation of enaminones and other electron-rich double bonds.[28,29] In Scheme 2, we propose a mechanism for the degradation of **5**, in which the radicals

[a] Abbreviations: PBS, phosphate-buffered saline solution; HepG2, hepatocellular carcinoma cells; B78-H1, amelanotic murine melanoma cells; MCF-7, breast cancer cells; HeLa, cervical cancer cells; 3-HBT, 3-hexylbenzo[*d*]thiazol-2(3*H*)-one; TBARS, malonyldialdehyde bound to thiobarbituric acid; 1) PagMDA, malonyldialdehyde.

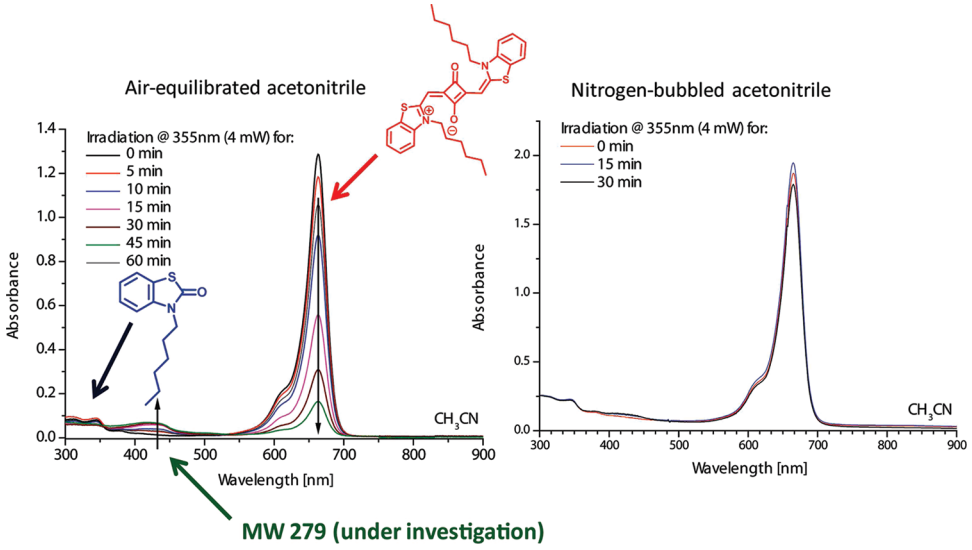

Figure 2. Change in the absorption spectra of **5** in air-equilibrated and nitrogen-bubbled acetonitrile upon irradiation with a laser source at 355 nm.

Table 1. Spectral Properties of the Mono- and Bis-squaraines **5** and **4** in Different Air-Equilibrated Solvents

solvent	$\lambda_{abs,max}$ [a] (ε_{max})	ε_{630} [b]	$\lambda_{em,max}$ [c]	Φ_f [d]
toluene, sq **4**	659 (88300)	73200	680	0.14
acetonitrile, sq **4**	628 (78200)	78100	667, 720	0.01
DMSO, sq **4**	647 (92000)	90600	680, 760	0.015
toluene, sq **5**	682 (295000)	35600	705	0.85
acetonitrile, sq **5**	663 (280000)	61000	675	0.21
DMSO, sq **5**	678 (301000)	53100	683	0.92

[a] Absorption maximum, in nm ± 0.5 nm, and maximum extinction molar coefficient, in L mol^{-1} cm^{-1}, ±10%. [b] Extinction molar coefficient at 630 nm, in L mol^{-1} cm^{-1}, ±10%. [c] Emission maximum, in nm ± 0.5. [d] Fluorescence quantum yield evaluated using zinc phthalocyanine in pyridine as standard, estimated error ± 10%.

that are formed can explain the phototoxicity of these molecules (vide infra). To further elucidate the nature and role of the photoproduced species, we performed a photodegradation reaction on an air-equilibrated acetonitrile solution containing **5** and limonene as the photooxidation target. Limonene is a particularly suitable substrate for such studies, as it gives different oxidation products, depending on the kind of ROS formed in solution (singlet oxygen, peroxides, or superoxides).[30] A solution containing squaraine **5** (2.5 mg, 0.04 mmol) and (*R*)-(+)-limonene (50 mg, 0.37 mmol) in acetonitrile (5 mL) was irradiated with a filtered white light halogen lamp (300 W) for 30 min. The reaction mixture was treated with $NaBH_4$ (25 mg, 0.66 mmol) to reduce any formed peroxide to the corresponding alcohol, according to Marine and Clemons.[31] The solution was then analyzed by GC-MS (Figure 3a). The oxidation products were identified by comparison with literature data, that is, using the NIST 05 database[32] (Table 2). The oxygenation of (*R*)-(+)-limonene provides a particularly sensitive fingerprint for the reactive intermediates. This substrate contains two oxidizable double bonds: one disubstituted and one trisubstituted. Photooxygenation by singlet oxygen yields products of oxidation at the trisubstituted double bond but not at the disubstituted double bond, which is not reactive. When we compared our results with those obtained by Foote et al.,[28−30] the photoreaction promoted by the squaraine is not in keeping with a singlet-oxygen mediated oxygenation. Table 3 shows the photooxidation products distribution in the photosensitized oxygenation of (*R*)-(+)-limonene.[28] Row 1 shows the percentage distribution of oxidized products expected for singlet oxygen reaction. Rows 2 and 3 show the observed product distribution for squaraine **5** and **4** photosensitization. The fact that the preponderance products are the two carveol derivatives **V** and **VI** and the appearance of **VII** brought us to conclude that the most likely mechanism involves the ablation of the allylic hydrogen by a radical species (either a ROS or a triplet carbonyl compound) and the reaction of the allyl radical with molecular oxygen to yield a peroxy radical. The latter can ablate the hydrogen of another limonene molecule to yield a hydroperoxide and an allyl radical according to a type I radical chain process.[12,13] The photochemical data collected are in agreement with the photophysical one. The encounter complex between squaraine and molecular oxygen can evolve by either photooxygenation of the enaminic bond in the squaraine backbone or ROS production (Supporting Information, S1). In both cases, the photogenerated products can then establish radical chain events (lipid peroxidation) that lead to type I cytotoxcity in cells. Interestingly, the same mechanism seems to describe the photooxigenation behavior of a number of cyanine-based photosensitizers (e.g., merocyanine 540, indocyanine green, and MKT-077).[33,34] We carried out the same photoxidation experiments on derivative **4** and observed the same product distribution (Figure 3b). The main difference between the two compounds is the reaction kinetics. The photoxidation observed in the case of **4** in much slower, probably due to the fact that the derivative **4** strongly aggregates in acetonitrile. In conclusion, our photooxidation studies demonstrate that the designed squaraines, when photoactivated, produce peroxide, allyl, and hydroperoxide radicals.

Phototoxicity and Mechanism of Photokilling of Squaraines. As the designed squaraines emit in the red, we used confocal microscopy to investigate whether they are taken up by cervical cancer cells (HeLa) cells. The images shown in Figure 4a have been obtained after the cells were treated for 4 h with **4** or **5**. It can be seen that both squaraines locate mainly in the cytoplasm: The punctuated distribution of the fluorescence may suggest that these compounds reside in

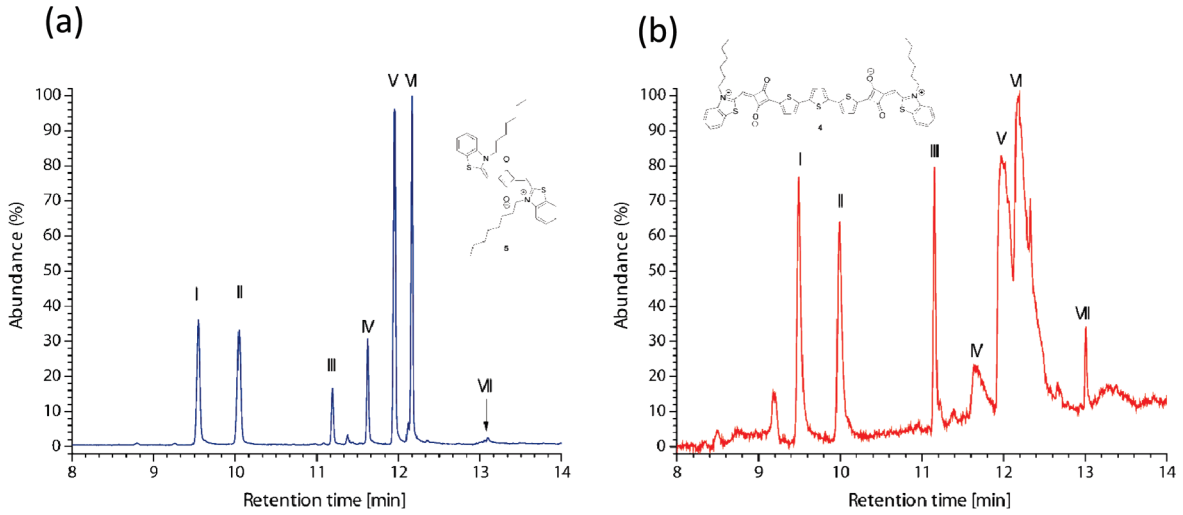

Figure 3. GC-MS chromatograms showing resolution of a solution of (*R*)-(+)-limonene in acetonitrile photosensitized by **5** (a) and **4** (b). Experimental details including column and GC conditions are given in the Experimental Section. Peak identification: I and II, either (1*S*,4*R*)- or (1*R*,4*R*)-1-methyl-4-(prop-1-en-2-yl)cyclohex-2-enol; III and IV, either (1*R*,5*S*)- or (1*S*,5*S*)-2-methylene-5-(prop-1-en-2-yl)cyclohexanol; V, (1*R*,5*S*)-2-methyl-5-(prop-1-en-2-yl)cyclohex-2-enol; VI, (1*S*,5*S*)-2-methyl-5-(prop-1-en-2-yl)cyclohex-2-enol; and VII, (*R*)-[4-(prop-1-en-2-yl)cyclohex-1-enyl]methanol (see Table 2).

Scheme 2. Proposed Mechanism for the Photodegradation of Squaraine **5**

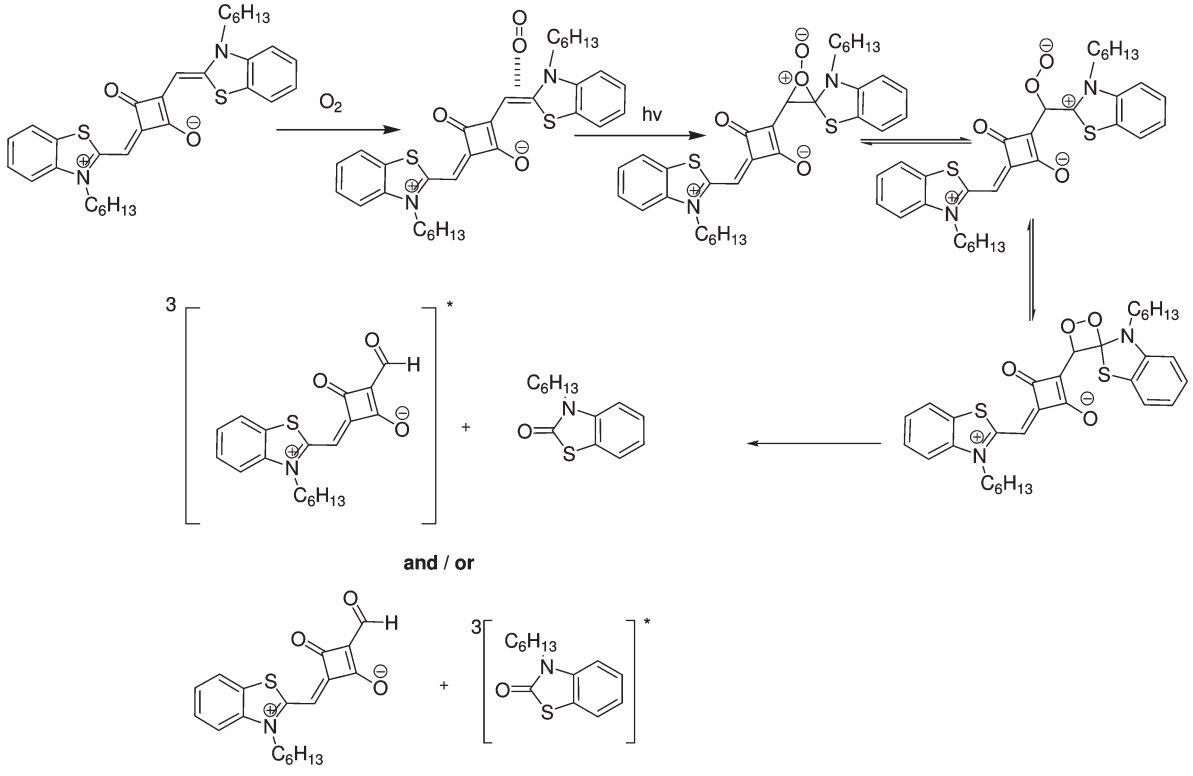

endocytotic vescicles and/or associate to the organelle membranes, through their double hydrocarbon chains. The fact that squaraines do not accumulate in the nucleus suggests that their potential to cause DNA damage, mutations, and carcinogenesis should be quite low.

The photodynamic effects promoted by the designed squaraines were tested in four cell lines: HeLa human cervical carcinoma, HepG2 human hepatic carcinoma, B78-H1 murine amelanotic clone derived from melanoma B16, and MCF-7 human breast cancer cell lines. An important property that a photosensitizer must possess is noncytotoxicity in the dark. We therefore evaluated the cytotoxicity of **4** and **5** in the dark as well as after irradiation, and the results obtained have been plotted together for comparison. Figure 4b shows that monosquaraine **5** is not cytotoxic in the dark at the concentrations used for PDT experiments: A limited cytotoxicity effect is observed at concentrations as high as 5 μM. Cytotoxicity effects were not observed neither in primary human vein endothelial cells (Huvec) nor when squaraine **5** was injected in mouse (3 μmol/kg, typical dose for PDT experiments) incorporated in small unilamellar liposomes of dioleoylphosphatidyl choline (Supporting

Table 2. Oxidation Products Obtained by the Photooxidation of Limonene with Squaraines **5** or **4**

peak	product	characteristic ions (*m*/*z*)	retention times (min)
I	(1*S*,4*R*)- or (1*R*,4*R*)-1-methyl-4-(prop-1-en-2-yl)cyclohex-2-enol	91, 119, 79, 134	9.55
II	(1*S*,4*R*)- or (1*R*,4*R*)-1-methyl-4-(prop-1-en-2-yl)cyclohex-2-enol	91, 119, 134, 79	10.05
III	(1*R*,5*S*)- or (1*S*,5*S*)-2-methylene-5-(prop-1-en-2-yl)cyclohexanol	91, 109, 134, 119	11.19
IV	(1*R*,5*S*)- or (1*S*,5*S*)-2-methylene-5-(prop-1-en-2-yl)cyclohexanol	91, 119, 134, 109	11.63
V	(1*R*,5*S*)-2-methyl-5-(prop-1-en-2-yl)cyclohex-2-enol	109, 91, 84, 119	11.95
VI	(1*S*,5*S*)-2-methyl-5-(prop-1-en-2-yl)cyclohex-2-enol	84, 91, 134, 119	12.17
VII	(*R*)-[4-(prop-1-en-2-yl)cyclohex-1-enyl]methanol	79, 91, 67, 55	13.09

Table 3. Photooxidation Products Distribution in the Photosensitized Oxygenation of (*R*)-(+)-Limonene[28] [a]

	limonene photooxidation products distribution (percentage)						
	I	II	III	IV	V	VI	VII
singlet oxygen sensitization[28]	10	34	19	23	9	4	0
photo- sensitization by **5**	17 + 16		5 + 9		25	26	1
photo- sensitization by **4**	11 + 11		6 + 6		29	33	2

[a] Row 1 shows the percentage distribution of oxidized products expected for singlet oxygen reaction. Rows 2 and 3 show the observed product distribution for squaraines **5** and **4** photosensitization.

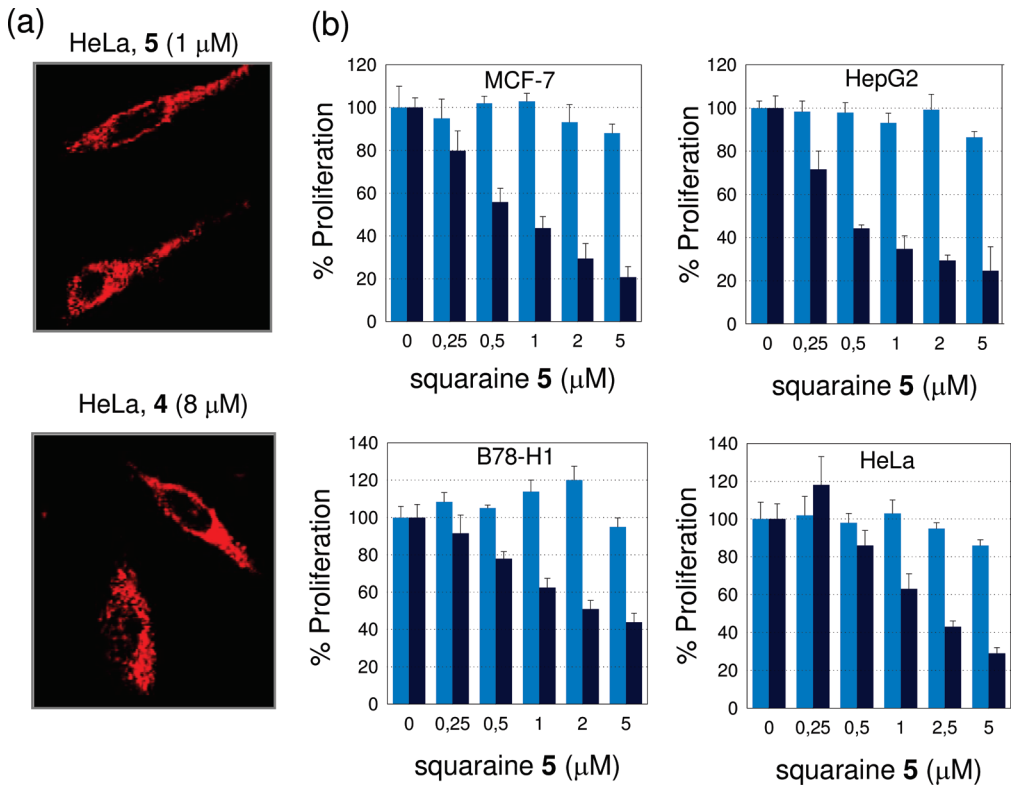

Figure 4. (a) Confocal laser microscopy images of HeLa cells treated for 4 h with squaraines **4** (8 μM) and **5** (1 μM). (b) Cytotoxicity of increasing amounts of squaraine **5** delivered to four different cancer cell lines either in the dark (light blue) or after light treatment (fluence rate, 15 J/cm^2) (dark blue). Viable cells were measured with a resazurine assay. Histograms report in ordinate the percent of relative proliferation, that is, the ratio $RFU_T/RFU_C \times 100$, where RFU_T is the fluorescence of treated cells, while RFU_C is the fluorescence of untreated cells. The data are the means ± SDs of three independent experiments.

Information, S2). In contrast, when squaraine **5** is photoactivated, it promotes a dramatic cytototoxic effect in all tested cancer cells (up to 80%). This experiment was carried out by treating the cells for 3 h with increasing amounts of **5**, followed by irradiation with a metal halogen lamp at a fluence of 15 J/cm^2, and 24 h after light treatment, a resazurine proliferation assay was carried out. As a control, we treated the cells with the same amount of DMSO present in the squaraine treatment (squaraines were dissolved in DMSO and diluted with cell medium; the final DMSO content was lower than 0.2%). Similar dose−response plots were also obtained with the bis-squaraine **4** (Supporting Information, S3). From these dose−response plots, we estimated the IC_{50} values reported in Table 4. The data obtained clearly indicate that **5** is a stronger photokilling agent than **4**: IC_{50} values of **4** (8−16 μM) are, depending on cell type, from 6 to 26 times higher than those of **5** (0.4−2 μM). The lower bioactivity of **4** is likely due to its capacity to aggregate in aqueous solution, as indicated by the UV spectra (Supporting Information, S4). Ramaiah et al.[7] reported that halogenated monosquaraines, irradiated at 34 J/cm^2, strongly

Table 4. IC_{50} Values Relative to Squaraines **4** and **5** Delivered to Cancer Cells[a]

	IC_{50} (μM)	
cells	squaraine **4**	squaraine **5**
HepG2	10.7	0.4
B78-H1	16.0	2.0
MCF-7	11.7	1.3
HeLa	8.1	1.3

[a] IC_{50} obtained by treating the cells for 3 h with the squaraines, followed by irradiation for 30 min (15 J/cm^2) and resazurine assay (24 h after irradiation).

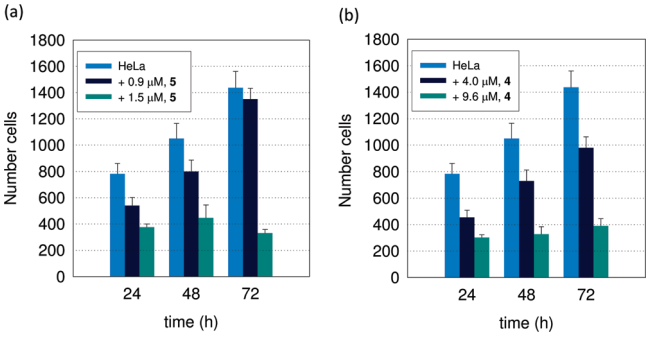

Figure 5. Phototoxicity of squaraines **5** (a) and **4** (b) in HeLa cells up to 72 h after light treatment (15 J/cm^2). Control are cells treated only with light.

inhibited the cloning efficiency of AS52 Chinese hamster ovary cells, with an estimated IC_{50} between 1 and 2 μM, rather similar to that observed with **5**. We also compared the phototoxicity of squaraine **5** with that of clinical mTHPC (Temoporfin) and found that the latter has IC_{50} values ~10-fold lower than the former, under the same conditions (not shown). Nevertheless, squaraine **5** can be considered as a promising PDT drug because it is phototoxic at relatively low concentrations ($\leq$1 μM), and it is not expected to cause the skin side effects typical of porphyrins.

As little is known about the photosensitizing properties of squaraines, we focused on this. First, we tested the antiproliferation effect of **4** and **5** in HeLa cells, up to 72 h following irradiation (Figure 5). When **4** and **5** are used at concentrations slightly higher than IC_{50} (1.5 μM for **5** and 9.6 μM for **4**), they completely arrest the growth over the entire range of time considered (72 h), whereas at lower doses they reduce the growth rate without completely stopping proliferation. Considering that squaraines **4** and **5** produce reactive peroxides upon photoactivation and that these molecules are expected to associate to the membranes through their hydrocarbon tails, we hypothesized that they could cause a lipid peroxidation injury by measuring the level of malonyldialdehyde (MDA) bound to thiobarbituric acid (TBARS),[35] in both untreated and photodynamically treated HeLa cells (Figure 6). As compared to untreated cells, which show a basal level of TBARS fixed to 100, treated cells (squaraine dose ~ IC_{50}, that is, 9.5 μM for **4** and 1.5 μM for **5**; fluence of 15 J/cm^2) show an increase of TBARS up to 4-fold, indicating that the photosensitizers cause a strong lipid peroxidation.[35] A similar behavior was observed with MCF-7 cells (Figure 6). To gain insight into the mechanism of photokilling triggered by the designed squaraines, we

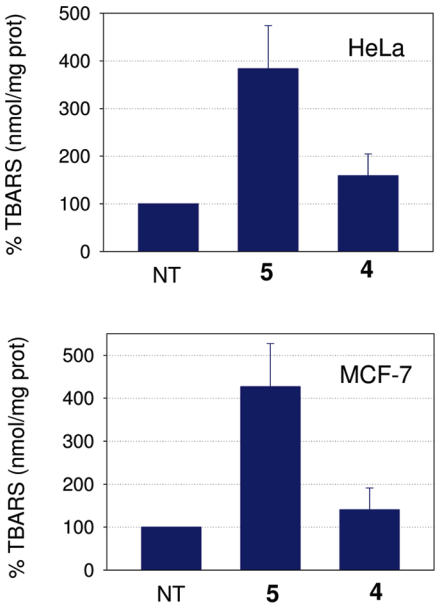

Figure 6. Level of TBARS in HeLa and MCF-7 cells treated photodynamically with squaraines **4** (9.6 μM) and **5** (1.8 μM). Ordinate reports the level of TBARS (nmol/mg protein) relative to that of untreated cells, which was fixed to 100.

investigated, by FACS, photodynamically treated HeLa cells stained with annexin V and propidium iodide (PI). In early apoptosis, cell membranes lose their phospholipid asymmetry, and phosphatidyl serine (PS), normally located in the inner leaflet, jumps into the outer leaflet. As annexin V shows a high affinity for PS, annexin V-FITC can mark the cells in early apoptosis. In contrast, necrotic cells, being permeable to annexin V and PI, are stained by both dyes.[36] Figure 7a shows a FACS analysis performed after irradiation (15 J/cm^2) of HeLa cells treated with **4** or **5**. When the squaraine concentration is lower than IC_{50}, the percentage of necrotic and apoptotic cells is very low (not shown), but at concentrations close to IC_{50} (9.5 μM for **4** and 1.5 μM for **5**), the fraction of cells in necrosis is nearly three times higher than the fraction of apoptotic cells, indicating that necrosis becomes the principal photokilling mechanism triggered by the squaraines. In the FACS experiment, the percentage of necrotic cells is not high because the analysis was performed only 30 min after light treatment, in an attempt to detect apoptotic cells. However, by means of a time-lapse experiment conducted over an interval of 72 h with living HeLa cells treated with **4** or **5** at a concentration close to IC_{50} and grown in a medium added with Hoechst (stains nuclei of living cells) and PI (stains nuclei of necrotic cells), we found that most cells die primarily by necrosis (Figure 7b). It can be seen that necrotic cells appear swelled up and stained in red because their membrane becomes permeable to PI. However, although in a limited percentage, there are also cells with an apoptotic morphology, characterized by shrinkage, membrane blebbing, and apoptotic bodies.[37] The activation of a caspase-dependent cell death pathway was confirmed by a caspase-3/7 assay performed at different times after PDT treatment (Figure 8). As the effector caspases 3 and 7 were found activated, the data confirmed the presence of apoptotic cells and suggest that the squaraines mediate a complex cell death pathway involving primarily necrosis but also apoptosis.

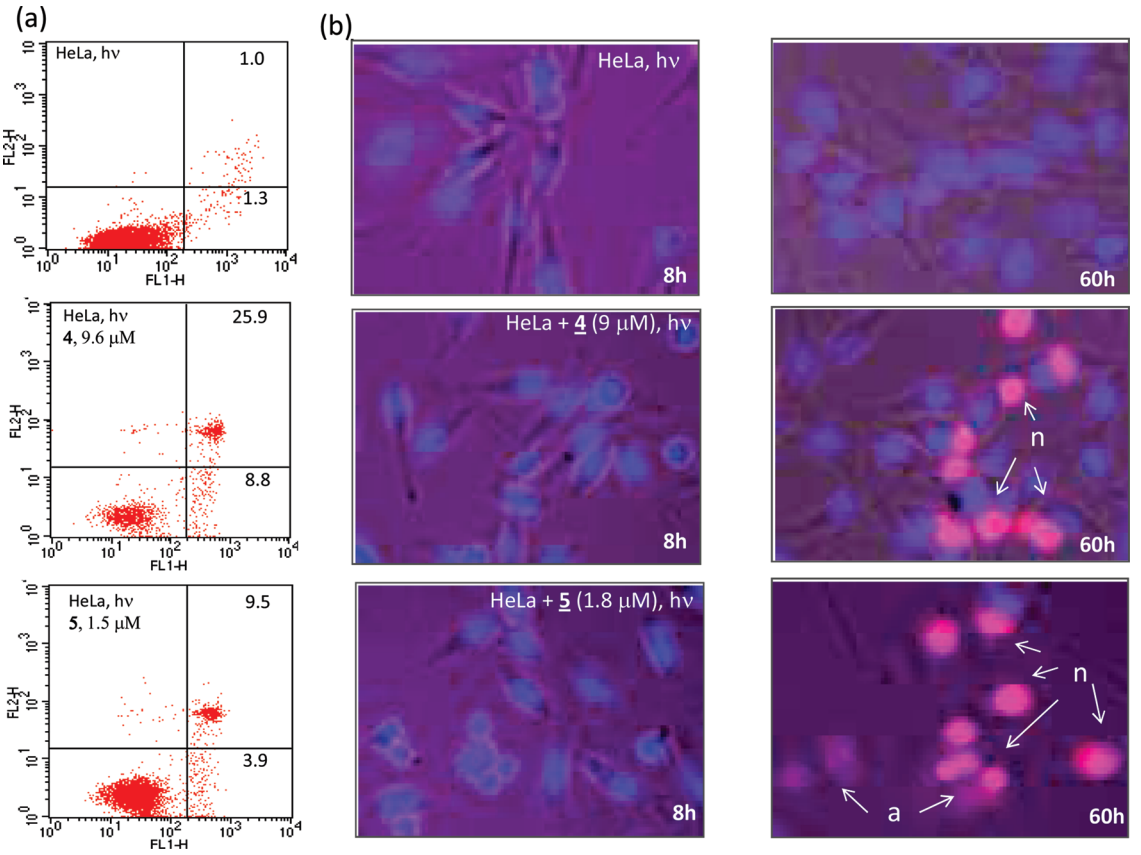

Figure 7. (a) FACS analysis of squaraine-treated HeLa cells photodynamically treated with **4** (9.6 μM) and **5** (1.5 μM) and stained with annexin V-FITC and PI. (b) Time-lapse experiment performed on living HeLa cells treated with Hoechst, PI, and **4** (9.6 μM) or **5** (1.5 μM). The images were obtained 8 and 60 h after treatment. As a control, the cells were not treated with the squaraiens (top panels). Red cells are necrotic, and blue cells are viable. Necrotic (n) and apoptotic (a) cells are indicated by white arrows.

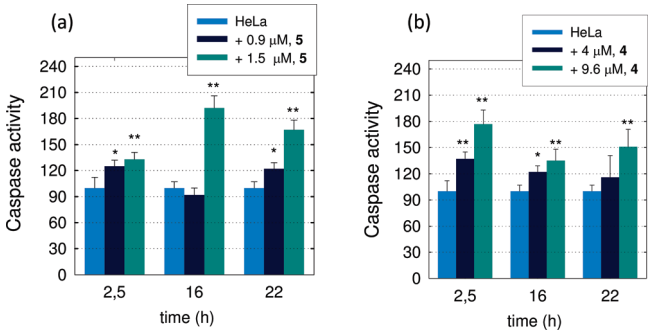

Figure 8. Caspases 3/7 activity in untreated or squaraine-treated HeLa cells. The cells were incubated with the squaraine **5** (a) or **4** (b) for 3 h and irradiation at a fluence of 15 J/cm^2. The caspase activity was measured with Apo-ONE TM caspase-3/7 assay. The data are the means ± SDs of at least two independent experiments. (*p < 0.05; **p < 0.01).

Conclusion

In this paper, we describe the synthesis of two π-extended squaraines, which, being characterized by a strong absorption between 550 and 750 nm, are potential photosensitizers in PDT. Upon irradiation, the designed squaraines undergo a phootooxidation process leading, through a type I phooto-process, to the formation of peroxide and hydroperoxide species. In the tested cells, these reactive species trigger a cell death primarily by necrosis. Confocal microscopy shows that these molecules efficiently internalize in HeLa cells where they accumulate in the cytoplasm. The squaraines induce a marked increase of MDA, which hints to lipid injury by peroxidation. In the dark, the squaraines are largely nontoxic, but when they are irradiated with light at a fluence of 15 J/cm^2, they promote a strong photodynamic effect that causes cell death in all tested cell lines. Monosquaraine **5** is found to be a stronger photosensitizer than bis-squaraine **4**. The results of this paper show that the synthesized squaraines, in particular **5**, represent a new class of therapeutic agent for PDT.

Experimental Section

Synthesis of 4,4′-(2,2′:5′,2″-Terthiophene-5,5″-diyl)bis(3-butoxycyclobut-3-ene-1,2-dione) (2). Under nitrogen atmosphere, a solution of 2,2′:5′,2″-terthiophene (0.65 g, 2.60 mmol) in anhydrous THF (100 mL) was added dropwise with a 1.6 M solution of butyllithium in *n*-hexane (2.6 mL) at 0 °C. Suddenly, a green-yellow precipitate was formed. After 30 min at room temperature, a second solution of 3,4-dibutoxycyclobut-3-ene-1,2-dione (0.81 g, 5.20 mmol) in anhydrous THF (5 mL) was added to the reaction mixture. The resulting red solution was stirred for 10 min and then poured into a saturated NH_4Cl solution (100 mL). After 30 min of stirring, the mixture was extracted with AcOEt (2 × 50 mL). The organic layer was dried over anhydrous Na_2SO_4, and then, the solvent was removed under reduced pressure. The residual red oil was taken up with cyclohexane to afford the pure product as a red precipitate that was collected by filtration (0.53 g, 0.96 mmol, 37%). ^{1}H NMR ($CDCl_3$): δ 7.78 (2H, d, J = 3.98 Hz), 7.32 (2H, d, J = 4.00 Hz), 7.26 (2H, s), 4.94 (4H, m), 1.92 (4H, m), 1.54 (4H, m), 1.03 (6H, m).

Synthesis of 4,4′-(2,2′:5′,2″-Terthiophene-5,5″-diyl)bis(3-hydroxycyclobut-3-ene-1,2-dione) (3). A solution of compound **2** (0.73 g, 1.32 mmol) in AcOH (30 mL) and water (15 mL) was

refluxed for 2 h in a mixture of 20 mL of AcOH and 1 mL of 10% HCl. After this period, the reaction mixture was cooled at ambient temperature. The red precipitate thus obtained was filtered off and washed directly on the filter with Et_2O to give the desired product as brown solid (0.53 g, 1.20 mmol, 91%). ^{1}H NMR (DMSO-d_6): δ 7.47 (2H, d, J = 3.77 Hz), 7.41 (2H, d, J = 4.03 Hz), 7.38 (2H, s).

Synthesis of Squaraine (4). A suspension of *N*-hexyl-2-methylbenzothiazolium iodide (0.195 g, 0.54 mmol) and the bis-semisquaraine **3** (0.119 g, 0.27 mmol) was suspended in a solution of 25 mL of BuOH, 5 mL of toluene, and 0.1 mL of pyridine. The red suspension was refluxed for 5 h under a Dean−Stark trap to azeotropycally remove the water formed. The reaction mixture was then cooled at 0 °C, and a golden brown precipitate was formed. The precipitate was isolated by suction filtration and washed directly on the filter with 20 mL of MeOH to give the pure title compound as a dark powder (0.160 g, 0.17 mmol, 64%); mp > 250 °C (dec). ^{1}H NMR (DMSO-d_6): δ 8.31 (2H, d, J = 7.91 Hz), 8.08 (2H, d, J = 8.47 Hz), 7.74 (2H, t, J = 7.87 Hz), 7.63 (2H, t, J = 7.64 Hz), 7.49 (2H, d, J = 3.84 Hz), 7.47 (2H, d, J = 3.75 Hz), 7.44 (2H, s), 6.64 (2H, s), 4.72 (4H, t, J = 6.26 Hz), 1.79 (4H, quint, J = 7.51 Hz), 1.47−1.36 (4H, m), 1.36−1.20 (8H, m), 0.90−0.80 (6H, m). Anal. calcd for $C_{48}H_{42}N_2O_4S_5 \cdot 7/2H_2O$: C, 61.71; H, 5.29; N, 3.00. Found: C, 61.78; H, 4.69; N, 2.83.

Spectroscopic Experiments. Steady-state UV/vis absorption spectra were recorded using a UV/vis/NIR Jasco V570 spectrometer. Steady-state emission spectra were recorded using a Jasco FP-6200 fluorometer. Fluorescence quantum yields (Φ_f) (Table 1) were determined by comparing the integrated emission intensity recorded upon irradiation of a standard of a sensitizer at a given wavelength to the integrated intensity obtained after irradiation of a standard, with a known quantum yield of fluorescence, at the same wavelength. The integrated intensities were recorded at different absorbances, and the slopes obtained were then used to obtain Φ_f. If the standard and the sensitizer were dissolved in different solvents, we accounted for differences in the light collection efficiency due to different refractive indexes, theoretically derived for a 90° angle setup, such as that in our fluorimeter:

$$\Phi_f = \Phi_f^{std}\left(\frac{slope_{sens}}{slope_{std}}\right)\left(\frac{n_{sens}}{n_{std}}\right)^2$$

Photobleaching and Photooxidation of Squaraines. Analysis of limonene photooxidized derivatives was carried out by GC-MS using a Clarus 500 instrument (PerkinElmer Instruments, Shelton, CT) equipped with a 30 m × 0.25 mm capillary column Elite-5MS (0.25 μm film thickness) (PerkinElmer). Helium was used as the carrier gas at a flow rate of 1 mL/min. The injector temperature was 250 °C, and the samples were injected in a splitless mode of injection. The oven temperature was set at 80 °C for 5 min, raised to 100 at 5 °C/min, held for 1 min, raised to 200 at 20 °C/min, and finally held for 3 min. The mass spectrometer was operated in the electron ionization mode (ionization energy of 70 eV). The source and transfer line temperatures were 160 and 180 °C, respectively. Detection was carried out in scan mode: m/z 50 to m/z 600. The limonene photooxidation protocol was as follows: (a) Fifty milligrams of limonene and 2.5 mg of the squaraine dye were dissolved in 5 mL of acetonitrile avoiding light exposure. (b) The mixture was illuminated for 30 min with a halogen lamp filtered below 500 nm (the white light coming from the 230 V, 300 W halogen lamp was filtered with a 3% by weight $K_2Cr_2O_7$ solution. The light coming out was completely absorbed for wavelengths below 500 nm). (c) The solution was dried under reduce pressure, and the remaining residue was dissolved in 3 mL of ethanol and cooled at 0 °C. A solution of $NaBH_4$ (25 mg) in ethanol (1 mL) was added to reduce the peroxides to alcohols, and the resulting mixture was stirred in the dark for 1 h. The mixture was poured in water, and the ethanol was removed at reduced pressure. The suspension obtained was extracted with 12 mL of *n*-hexane and dried over Na_2SO_4. The dried solution was filtered and injected in the GC-MS apparatus.

Cell Proliferation Assay. The percentage of viable cells was determined by the resazurine assay following the manufacturer's instructions (Sigma-Aldrich, Milan, Italy). The values were obtained by spectrofluorometer Spectra Max Gemini XS (Molecular Devices, Sunnyvale, CA). To reach the plateau phase growth, defined cell densities were seeded in a 96-multiwell plate: HeLa 5000 cells/well, HepG2 7000 cells/well, B78-H1 5000 cells/well, and MCF-7 7000 cell/well.

Apo-ONE Caspase-3/7 Homogeneous Assay. The Apo-ONE casapase-3/7 homogeneous assay (Promega, Milano, Italy) was used to measure the activity of caspase-3/7. Following the manufacturer's instructions, the cells were grown in a 96-well plate (density of 5000 cells/well) and exposed to **4** and **5** light treatment. The assay was performed at different times (2.5, 16, and 22 h) following light activation. Homogeneous caspase-3/7 reagent (substrate was dilute 1:100 with provided buffer) was added, maintaining a 1:1 ratio of reagent to sample. The measure of fluorescence of each well was read at an excitation wavelength of 485 ± 20 nm and an emission wavelength of 530 ± 25 nm (Spectra Max Gemini XS, Molecular Devices Corp., CA).

Lipid Peroxidation (TBARS Assay). HeLa cells were photodynamically treated with **4** or **5**. Twenty-four hours after treatment, the cells were washed with phosphate-buffered saline solution (PBS), trypsinized, and pelleted. The pellets (10^6 cells) were suspended in 2 mL of 0.9% NaCl and vortexed vigorously, and an aliquot was taken from each sample for a Lowry protein assay. The remaining samples were added with 230 μL of trichloroacetic acid-saturated solution (250 g of trichloroacetic acid in 100 mL of water), vortexed, and centrifuged at 3000*g* (10 min) to precipitate the proteins. The supernatants (1.6 mL) were placed in glass test tubes, and 200 μL of 14.4 mg/mL 2-thiobarbituric acid in 0.1 N NaOH solution were added. The samples were incubated for 45 min at 75 °C. Standards were prepared from the hydrolysis of 1,1,2,2-ethoxypropane in a 40% trichloroacetic acid solution. After the samples were cooled, the absorbances of the samples were read at 535 nm by Spectrophotometer Ultrospec 1100 Pro (Amersham Pharmacia Biotech, Cambridge, United Kingdom) Thiobarbituric acid reactive substances (TBARS) values were calculated as nmol/mg of total protein.[35]

FACS Analysis. Apoptosis was assessed using annexin V, a protein that binds to phosphatidylserine (PS) residues, which are exposed on the cell surface of apoptotic cells. The cells were plated in a six-well plate at density of 5×10^5 cells/well. One day after, the cells were treated with **4** and **5** for 3 h and illuminated for 30 min. After light activation, the cells were washed with PBS, trypsinized, and pelleted. The pellets were suspended in 100 μL of Hepes buffer with 2 μL of Annexin V and 2 μL of PI (annexin-V FLUOS Staining kit, catalog no. 11858777001, Roche, Penzberg, Germany) and incubated for 10 min at 25 °C in the dark. Cells were immediately analyzed by FACScan (Becton-Dickinson, San Jose, United States). A minimum of 10000 cells for sample was acquired in list mode and analyzed using Cell Quest software. The cell population was analyzed by FSC light and SSC light. The signal was detected by FL1 (annexin-V-FLUOS) and FL-2 (PI). The dual parameter dot plots combining annexin V-FITC and PI fluorescence show the vial cell population in the lower left quadrant (annexinV−PI−), the early apoptotic cells in the lower right quadrant (annexin V+PI−), and the late apoptotic or necrotic cells in the upper right quadrant (annexinV+PI+).

Confocal Microscopy. To study the uptake, HeLa cells were plated (2×10^5) on coverslips (diameter 24 mm) and after 24 h treated with squaraine **4** or **5** for 3 h. The cells were illuminated with a metal halogen white lamp at a fluence of 15 J/cm^2. Four hours after photoactivation, the glasses were prepared. The cells were washed twice with PBS and fixed with 3% paraformaldehyde (PFA) in PBS for 20 min. After the cells were washed with

0.1 M glycine, containing 0.02% sodium azide in PBS, to remove PFA and Triton X-100 (0.1% in PBS), the cells were incubated with Hoechst to stain the nuclei. The cells were analyzed using a Leica TCS SP1 confocal imaging system.

Time-Lapse. The HeLa cells were plated at density of 2.5×10^5 cells in a six-well plate. The day after, the cells were treated with squaraine **4** or **5**. After photoactivation, the medium was removed and substitued with fresh medium containing Hoechst and PI (both at 2 μg/mL) to detect necrotic and apoptotic cells. Samples were placed in a temperature (37 °C) and 5% CO_2-controlled coverslip holder of the microscope. The time-lapse experiment was documented by serial images obtained with a Leica AF6000 LX (Leica Microsystems, Heidelberg, Germany).

Acknowledgment. This work has been carried out with the financial support of FVG-2008, PRISMA 2007, and PRIN 2007.

Supporting Information Available: Information about (i) photooxidation of squaraines **4** and **5**, (ii) a brief description of the in vivo toxicity experiment, (iii) dose−response plots of squaraine **4** in different cancer cell lines, and (iv) the absorption spectra of squaraines **4** and **5** in water. This material is available free of charge via the Internet at http://pubs.acs.org.

References

(1) Sprenger, G. E.; Ziegenebein, W. Cyclobutenediylium Dyes. *Angew. Chem., Int. Ed. Engl.* **1968**, *7*, 530–535.
(2) Maahas, G.; Hegenberg, P. Syntheses and derivatives of squaric acid. *Angew. Chem., Int. Ed. Engl.* **1966**, *5*, 888–893.
(3) Keil, D.; Hartmann, H. Synthesis and characterization of a new class of unsymmetrical squaraine dyes. *Dyes Pigm.* **2001**, *49*, 161–179.
(4) Schmidt, A. H. *Oxocarbons*; West, R., Ed.; Academic Press: New York, 1980; p 185.
(5) Santos, P. F.; Reis, L. V.; Almeida, P.; Serrano, J. P.; Oliveira, A. S.; Vieira-Ferreira, L. F. Efficiency of single oxygen generation of aminosquarylium cyanines. *J. Photochem. Photobiol., A* **2004**, *163*, 267–269.
(6) Ramaiah, D.; Eckert, I.; Arun, K. T.; Weidenfeller, L.; Epe, B. Squaraine dyes for photodynamic therapy: Study of their cytotoxicity and genotoxicity in bacteria and mammalin cells. *Photochem. Photobiol.* **2002**, *76*, 672–677.
(7) Ramaiah, D. A.; Joy, N.; Chandrasekar, N. V.; Eldho, S. D.; George, M. V. Halogenated squaraine dyes as potential photochemotherapeutic agents. Synthesis and study of photophysical properties and quantum efficiencies of single oxygen generation. *Photochem. Photobiol.* **1997**, *65*, 783–790.
(8) Ramaiah, D.; Eckert, I.; Arun, K. T.; Weidenfeller, L.; Epe, B. Squaraine dyes for photodynamic therapy: Mechanism of cytotoxicity and DNA damage induced by halogenated squaraine dyes plus light (> 600 nm). *Photochem. Photobiol.* **2004**, *79*, 99–104.
(9) Sreejith, S.; Divya, K. P.; Ajayaghosh, A. A near-infrared squaraine dye as a latent ratiometric fluorophore for the detection of aminothiol content in blood plasma. *Angew. Chem., Int. Ed. Engl.* **2008**, *47*, 7883–7887.
(10) Dolmans, D. E.; Fukumura, D.; Jain, R. K. Photodynamic therapy for cancer. *Nat. Rev. Cancer* **2003**, *3*, 380–387.
(11) Castano, A. P.; Mroz, P.; Hamblin, M.R.. Photodynamic therapy and anti-tumour immunity. *Nat. Rev. Cancer* **2006**, *6*, 535–545.
(12) Dougherty, T. J.; Gomer, C. J.; Henderson, B. W.; Jori, G.; Kessel, D.; Korbelik, M.; Moan, P.; Peng, Q. Photodinamic Therapy. *J. Natl. Cancer Inst.* **1998**, *90*, 889–905.
(13) Miller, J. Chemistry behind the News—Photodynamic Therapy: The Sensitization of Cancer Cells to Light. *J. Chem. Educ.* **1999**, *76*, 592–594.
(14) Pervaiz, S. Reactive oxygen-dependent production of novel photochemotherapeutic agents. *FASEB J.* **2001**, *15*, 612–617.
(15) Josefsen, L. B.; Boyle, R. W. Photodynamic therapy and the development of metal-based photosensitisers. *Met. Based Drugs* **2008**, 276109–276133.
(16) Castano, A. P.; Demidova, T. N.; Hamblin, M. R. Mechanisms in photodynamic therapy: Part one-photosensitizers, photochemistry and cellular localization. *Photodiagn. Photodyn. Ther.* **2004**, *1*, 279–293.
(17) Castano, A. P.; Demidova, T. N.; Hamblin, M. R. Mechanisms in photodynamic therapy: part three-photosensitizers pharmacokinetics, biodistribution, tumor localization and modes of tumor destruction. *Photodiagn. Photodyn. Ther.* **2005**, *2*, 91–106.
(18) Allison, R. R.; Downie, G. H.; Cuenca, R.; Hu, X. H.; Childs, C. J.; Sibata, C. H. Photosensitizers in clinical PDT. *Photodiagn. Photodyn. Ther.* **2004**, *1*, 27–42.
(19) Sessler, J. L.; Miller, R. A. Texaphyrins: New drugs eith diverse clinical applications in radiation and photodynamic therapy. *Biochem. Pharmacol.* **2000**, *59*, 733–9.
(20) Comuzzi, C.; Cogoi, S.; Overhand, M.; van der marel, G. A.; Overkleeft, H. S.; Xodo, L. E. Synthesis and biological evaluation of new pentaphyrin macrocycles for photodynamic therapy. *J. Med. Chem.* **2006**, *49*, 196–204.
(21) Rapozzi, V.; Lombardo, C.; Cogoi, S.; Comuzzi, C.; Xodo, L. E. Small interfering RNA-mediated silencing of glutathione S-transferasi A1 sensitizes hepatic carcinoma cells to photodynamic therapy with pentaphyrins. *ChemMedChem* **2008**, *3*, 565–568.
(22) Rapozzi, V.; Miculan, M.; Xodo, L. E. Evidence that photoactivated pheophorbide *a* causes in human cancer cells a photodynamic effect involving lipid peroxidation. *Cancer Biol. Ther.* **2009**, *14*, 1–10.
(23) Taquet, J. P.; Frochot, C.; Manneville, V.; Barberi-Heyob, M. Phthalocyanines covalently bound to biomolecules for a targeted photodynamic therapy. *Curr. Med. Chem.* **2007**, *14*, 1673–1687.
(24) Juarranz, A.; Jaen, P.; Sanz-Rodriguez, F.; Cuevas, J.; Gonzales, S. Photodynamic therapy of cancer. Basic principles and applications. *Clin. Transl. Oncol.* **2008**, *10*, 148–154.
(25) Josefsen, L. B.; Boyle, R.W. Photodynamic therapy: Novel third-generation photosensitizers one step closer? *Br. J. Pharmacol.* **2008**, *154*, 1–3.
(26) Gayathri Devi, D.; Cibin, T. R.; Ramaiah, D.; Abraham, A. J. Bis (3,5-diiodo-2,4,6-trihydroxyphenyl) squaraine: a novel candidate in photodynamic therapy for skin cancer models in vivo. *Photochem. Photobiol., B* **2008**, *92*, 153–159.
(27) Yagi, S.; Ohta, T.; Akagi, N.; Nakazumi, H. The synthesis and optical properties of bis-squarylium dyes bearing arene and thiophene spacers. *Dyes Pigm.* **2008**, *77*, 525–536.
(28) Foote, C. S.; Lin, J. W.-P. Chemistry of singlet oxygen. VI. Photooxygenation of enamines: Evidence for an intermediate. *Tetrahedron Lett.* **1968**, *9* (29), 3267–3270.
(29) Mazur, S.; Foote, C. S. Chemistry of singlet oxygen. IX. Stable dioxetane from photooxygenation of tetramethoxyethylene. *J. Am. Chem. Soc.* **1970**, *92* (10), 3225–3226.
(30) Foote, C.; Wexler, S.; Ando, W. Chemistry of Singlet Oxygen. III. Product Selectivity. *Tetrahedron Lett.* **1965**, *46*, 4111–4118.
(31) Marine, S.; Clemons, J. Determination of limonene oxidation products using SPME and GC-MS. *J. Chromatogr. Sci.* **2003**, *41* (1), 31–35.
(32) Mikaia, A.; Stein, S. E.; Zaikin, V.; Zhu, D.; Milman, B.; Babishok, V.; Zenkevich, I.; Linstrom, P.; Mirokhin, Y.; Tchekhovskoi, D.; Mallard, W. G.; Sparkman, O. D.; Sparkman, J. A. *NIST/EPA/NIH Mass Spectral Library—Version 2.0d*; National Institute of Standards and Technology: Gaithersburg, MD, 2005.
(33) Kawakami, M.; Suzuki, M.; Kawai, H.; Ogawa, K.; Shishido, T. A self-sensitized photoreaction of rhodacyanine dye, MKT 077. *Tetrahedron Lett.* **1998**, *39* (13), 1763–1766.
(34) Hoebeke, M.; Piette, J.; van de Vorst, A. Photosensitized production of singlet oxygen by merocyanine 540 bound to liposomes. *J. Photochem. Photobiol., B: Biol.* **1991**, *9* (3−4), 281–294.
(35) Wong, S. H. Y.; Knight, J. A.; Hopfer, S. M.; Zaharia, O.; Leach, C. N.; Sunderman, F. W. Lipoperoxides in plasma as measured by liquid-chromatographic separation of malondialdehyde-thiobarbituric acid adduct. *Clin. Chem.* **1987**, *33*, 214–220.
(36) Koopman, G.; Reutelingsperger, C. P. M.; Kuijten, G. A. M.; Keehnen, R. M. J.; Palsvan, S. T.; Oers, M. H. J. Annexin V for flow cytometric detection of phosphatidylserine expression on B cells undergoing apoptosis. *Blood* **1994**, *84*, 1415–1420.
(37) Ziegler, U.; Groscurth, P. Morphological features of cell death. *News Physiol. Sci.* **2004**, *19*, 124–128.